

μ Dose: a compact system for environmental radioactivity and dose rate measurement

Konrad Tudyka^a, Sebastian Miłosz^a, Grzegorz Adamiec^a, Andrzej Bluszcz^a, Grzegorz Poręba^a, Łukasz Paszkowski^b, Aleksander Kolarczyk^b

^a*Silesian University of Technology, Institute of Physics - Centre for Science and Education, Division of Radioisotopes, ul. S. Konarskiego 22B, 44-100 Gliwice, Poland*

^b*AKOTECH, ul. Cypriana Norwida 6/10, 41-700 Ruda Śląska, Poland*

Abstract

μ Dose is a novel compact analytical instrument for assessing low level ^{238}U , ^{235}U , ^{232}Th decay chains and ^{40}K radioactivity. The system is equipped with a dual α/β scintillator allowing discrimination between α and β particles. The unique built-in pulse analyzer measures the amplitude of each individual pulse, its shape and the time interval between subsequent pulses. This allows the detection of pulse pairs arising from subsequent decays of $^{214}\text{Bi}/^{214}\text{Po}$, $^{220}\text{Rn}/^{216}\text{Po}$, $^{212}\text{Bi}/^{212}\text{Po}$ and $^{219}\text{Rn}/^{215}\text{Po}$. The obtained α and β counts and four separate decay pair counts are used to calculate ^{238}U , ^{235}U , ^{232}Th and ^{40}K specific activities in measured samples through the use of radioactivity standards. The μ Dose system may be equipped with various photomultipliers and counting containers to assess radionuclide concentrations of samples of masses ranging between 0.4 g and 4 g. As a result, the user can customize the system to their needs and maximize the instrument's performance. The system is controlled by dedicated software with a graphical user interface and modules for system calibration, data visualization, specific radioactivity calculations and dose rate determination using the infinite matrix assumption.

Keywords: decay pairs, environmental radioactivity, uranium, thorium, potassium, dose rate

1. Introduction

In trapped charge dating (optically stimulated luminescence, thermoluminescence, electron spin resonance) age is determined from the equivalent total absorbed radiation dose and radiation dose rate. In the natural environment radiation dose rate arises from ^{238}U , ^{235}U , ^{232}Th decay chains and ^{40}K . Commonly this is assessed using - field instruments, and laboratory analysis of samples including thick source alpha counting, thick source beta counting, high resolution gamma spectrometry, alpha spectrometry,

Email addresses: konrad.tudyka@polsl.pl (Konrad Tudyka), aleksander.kolarczyk@udose.eu (Aleksander Kolarczyk)

mass spectrometry, flame photometry, inductively coupled plasma mass spectrometry, neutron activation, X-ray fluorescence and other techniques.

Thick source alpha counting (TSAC) has been developed by Turner et al. (1958) to provide a relatively easy and inexpensive way of assessing the low level content of alpha emitters in biological tissues. Later this technique was adapted to determining the uranium and thorium content in samples of fired ceramics for assessing the annual dose for luminescence dating by Aitken (1985). In TSAC, the powdered sample is placed on a plastic sheet coated with a very thin layer of the scintillator ZnS:Ag attached to its surface. Alpha particles, emitted by U and Th series members, upon reaching the screen produce scintillations with practically 100% efficiency. In order to estimate the contribution from the U and Th series, additionally the so-called slow and sometimes fast pairs are counted. Such pairs are fast successions of counts due to the short lived ^{216}Po ($t_{1/2} = 0.145$ s) in the ^{232}Th series and ^{215}Po ($t_{1/2} = 1.78$ ms) in the ^{235}U series (Aitken, 1985). Today the TSAC technique is widely used (Cawthra et al., 2018; Chen et al., 2015; Duller et al., 2015; Fu et al., 2017; Jankowski et al., 2016; Kühn et al., 2017; Sabtu et al., 2015; Schmidt et al., 2017) for assessing the annual dose in trapped charge dating techniques. However, there are some significant limitations in the conventional TSAC technique. For example, the activity of ^{40}K which is a major dose contributor to the dose rate in environmental samples, cannot be determined using this technique and an independent determination by different means is usually performed (Dunseth et al., 2017; Jacobs et al., 2016; Junge et al., 2016; Roettig et al., 2017). Additionally, the ^{238}U decay chain may cause problems due to possible disequilibrium (Eitrheim et al., 2016; Krbetschek et al., 1994; Prescott and Hutton, 1995). Another drawback is the influence of sample's reflectance on the TSAC efficiency (Huntley, 1978) which can cause up to 6% error in an apparatus setting proposed by Aitken (1985).

In addition to the TSAC technique an alternative method of β counting was proposed by Sanderson (1988). This is a much more rapid technique of annual dose rate determination, however it cannot assess the specific radioactivities of ^{238}U , ^{235}U , ^{232}Th decay chains or ^{40}K (Sanderson, 1988; Bøtter-Jensen and Mejdahl, 1988).

In the current work, we describe a novel system - μ Dose - that opens up new possibilities and largely removes limitations described in the previous paragraphs. This is done through the employment of a dual α/β scintillator module, a new measurement setup, a new pulse analyzer unit (Miłosz et al., 2017), and advanced data processing. The system allows detection of two β/α decay pairs in addition to the above mentioned α/α pairs. The first pair arises in the ^{232}Th series from subsequent decays of ^{212}Bi and ^{212}Po where ^{212}Po has a half-life of 299 ns. The second β/α pair arises in the ^{238}U series from subsequent decays of ^{214}Bi and ^{214}Po where ^{214}Po has a half-life of 164 μs . Therefore, four decay pairs can be used to assess the specific activity of thorium and uranium decay chains as well as the potassium activity.

The μ Dose system is designed with emphasis on natural radioactivity measurement and the software is equipped with modules for dose rate measurement that is dedicated to trapped charge dating. With some modifications the system may be adapted for other purposes as well.

In the following sections we provide a detailed description of the μ Dose system, its performance, decay chain activity measurement method and the ^{40}K assessment.



Figure 1: The μ Dose system.

2. Experimental Section

2.1. System construction

μ Dose is a very compact system (shown in Fig. 1) as it takes just over 20 cm \times 20 cm of desk space and 35 cm height. The entire electronics, including a stable high voltage power supply, a photomultiplier and a pulse analyzer are built into the system and no additional components except a PC (which can control several such devices) are required for system operation. In the μ Dose system, the sample is placed in a dedicated sample container which is placed below the photomultiplier (Fig. 2). The container is equipped with a reusable dual (sandwich) α and β scintillator module covered by a 0.2 μ m replaceable silver foil on the underside of the scintillator. The silver foil is easily penetrated by β and the vast majority of α particles emitted by the sample. The silver layer increases the number of photons that reach the photomultiplier (PMT) and it also removes the measurement variability that arises from the sample's reflectance because scintillation photons are reflected from the silver layer rather than the sample. The sample container is gas-tight to prevent radon migration from and into it. The sample itself has a geometry of a thin disk which matches the diameter of the photocathode. Depending on the expected sample mass, the system can accommodate PMT's which have photocathode diameter from 30 up to 70 mm.

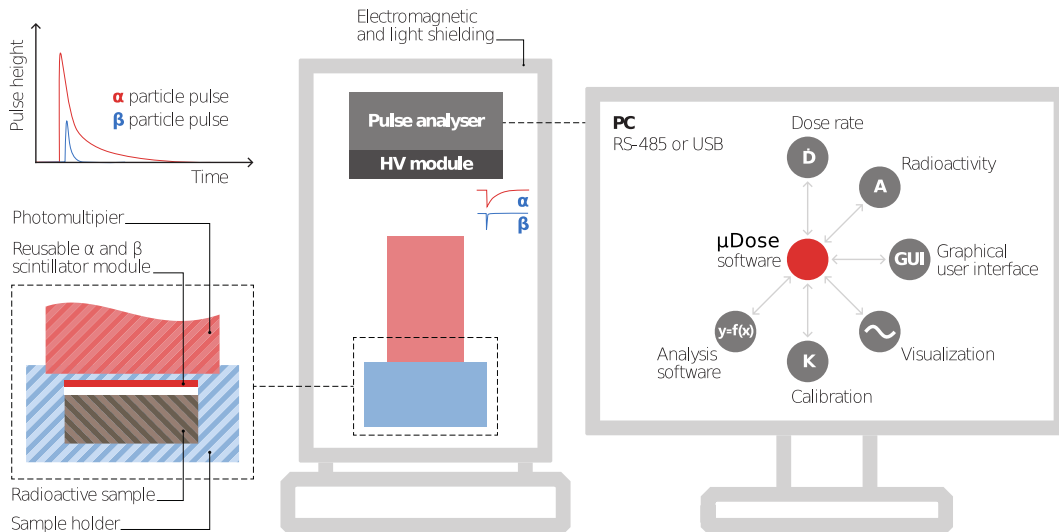


Figure 2: Block diagram of the μ Dose system.

2.2. Electronics

The pulse analyzer has been described in detail in Miłosz et al. (2017), therefore here only a brief description is given. The α and β particles produce scintillations in two different scintillator layers. The generated pulse shapes are different for each of the two scintillators, permitting the identification of the source particle of each pulse. This shape is preserved by the PMT and amplifier where the scintillations are transformed into electrical pulses and significantly amplified. The pulse analyzer detects the incoming voltage pulses (Fig. 2) and stores them as series of ADC values that represent each pulse. These pulse data are time-stamped and stored for further processing. The acquired data are then transferred to the computer and processed by a dedicated algorithm that determines the pulse height, the pulse shape and the time when each pulse appeared. The pulse height and the pulse shape allow to discriminate between α and β induced pulses. In addition, the algorithm is also capable of identifying pulses that do not match neither α nor β particles (Tudyka et al., 2017) enabling the removal of background pulses arising from electrical noise or other interfering sources. The software also deconvolutes piled up pulses from decays that appeared within a small time interval (ca. 100 ns).

The electronics module has a built-in high stability, low ripple, high voltage supply. This is controlled and monitored for system stability by the software. To protect the PMT, the high voltage is automatically switched off when the drawer with the sample container is opened.

2.3. α , β and decay pairs detection

Fig. 3 shows a typical 2D pulse height vs. pulse shape histogram where the colour indicates relative frequency of the recorded pulses obtained from sample 1 with artificial ^{238}U , ^{235}U , ^{232}Th decay chains and ^{40}K concentrations (see paragraph "Samples and sample preparation" for detailed description).

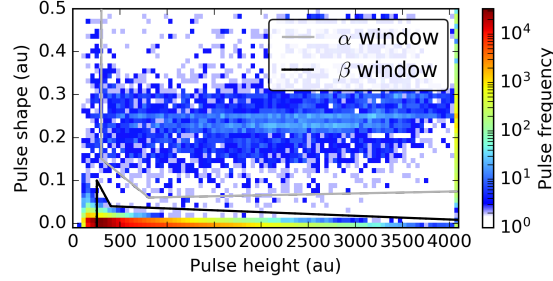


Figure 3: Data for a sample no. 1 (see section 3.1) measured for 44 hours. 2D pulse height vs. pulse histogram where the colour indicates relative frequency of appearance of the pulses. The α window is marked with the grey line above ca. 0.1 au pulse shapes parameter, the β window is marked with the black line below the α window. Note that beyond the α window there are pulses whose height exceeds 4000 au.

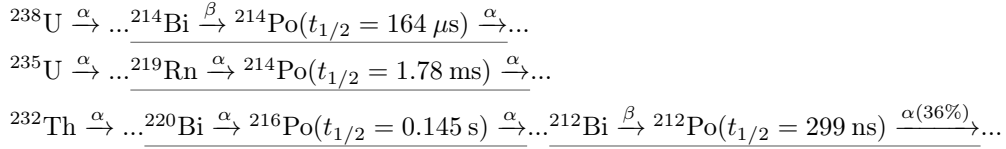


Figure 4: The sections of ${}^{238}\text{U}$, ${}^{235}\text{U}$ and ${}^{232}\text{Th}$ decay chains where the decay pairs occur showing relevant decay modes, half-lives and the branching ratio where relevant.

In environmental samples, of typically $100\text{--}1000 \text{ Bq}\cdot\text{kg}^{-1}$ total activity concentration, uncorrelated decays would be detected at a rate of $< 1 \text{ s}^{-1}$. However, as can be seen in diagram (Fig. 4), some radionuclides in the natural decay chains have half-lives significantly less than 1 s, which would result in correlated decays with much shorter time intervals observed as two pulses being detected in quick succession, so-called decay pairs. Since μ Dose detects and identifies both α and β particles, the system can identify and count the two α - α decay pairs used in TSAC (${}^{220}\text{Rn}/{}^{216}\text{Po}$, ${}^{219}\text{Rn}/{}^{215}\text{Po}$) and also two β - α decay pairs (${}^{212}\text{Bi}/{}^{212}\text{Po}$, ${}^{214}\text{Bi}/{}^{214}\text{Po}$). To detect those decay pairs the system builds a time interval distribution from the recorded time intervals between events classified as β pulses followed in quick succession of an α pulse (Fig. 5a, b and c). This reveals the exponential function arising from ${}^{212}\text{Bi}/{}^{212}\text{Po}$ (Fig. 5a) and ${}^{214}\text{Bi}/{}^{214}\text{Po}$ (Fig. 5b) decay pairs. Similarly, time interval distribution between events classified as α (Fig. 5d, e and f) allow to reveal the exponential decay arising from ${}^{219}\text{Rn}/{}^{215}\text{Po}$ (Fig. 5d) and ${}^{220}\text{Rn}/{}^{216}\text{Po}$ (Fig. 5e) decay pairs. Fig. 5c and f show remaining β - α and α - α time intervals arising from random decays. On each inset in Fig. 5, the fitted signal (sig) and background (bg) are marked. Note that background in Fig. 5a, b, c, f is virtually absent.

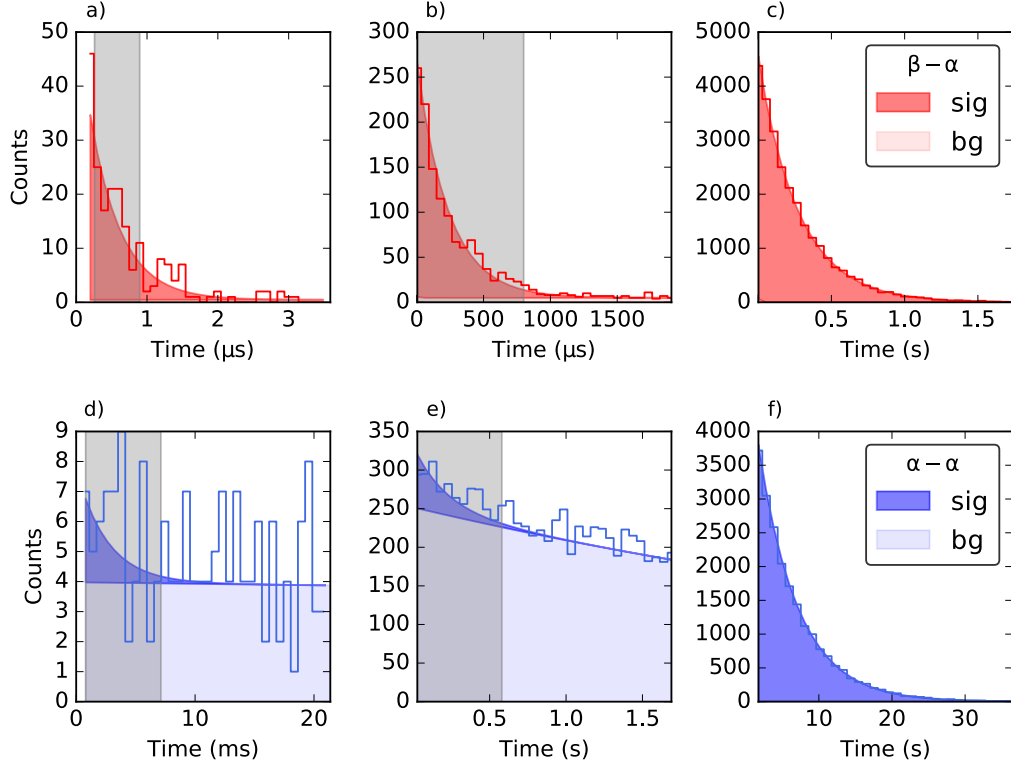


Figure 5: Data for sample no. 1 measured for 44 hours. Distributions for β - α time intervals in ranges a) 0-3.6 μ s, b) 3.6-2100 μ s, c) > 2100 μ s and α - α time intervals in ranges d) 0.5-21 ms, e) 21 ms - 1.7 s, c) > 1.7 s. Measured time intervals are shown by the stepped lines, the fitted signal (s) and background (b) are depicted by the filled areas. a), b), d) and e) plots reveal subsequent decays of $^{220}\text{Rn}/^{216}\text{Po}$, $^{219}\text{Rn}/^{215}\text{Po}$, $^{212}\text{Bi}/^{212}\text{Po}$ and $^{214}\text{Bi}/^{214}\text{Po}$, respectively. d) and g) show remaining, purely random β - α and α - α time interval distributions. Note the differing horizontal axis scales on plots a-f.

2.4. ^{238}U , ^{235}U , ^{232}Th and ^{40}K activity assessment

The four decay pairs count rates can be used to directly determine the activity per unit of mass

$$\begin{aligned} r_{\text{Bi-212/Po-212}} &= k_{\text{Bi-212/Po-212}} a_{\text{Bi-212/Po-212}}, \\ r_{\text{Bi-214/Po-214}} &= k_{\text{Bi-214/Po-214}} a_{\text{Bi-214/Po-214}}, \\ r_{\text{Rn-220/Po-216}} &= k_{\text{Rn-220/Po-216}} a_{\text{Rn-220/Po-216}}, \\ r_{\text{Rn-219/Po-215}} &= k_{\text{Rn-219/Po-215}} a_{\text{Rn-219/Po-215}}. \end{aligned} \quad (1)$$

Here r are the net count rates of decay pairs indicated in subscripts, k are calibration parameters for the given system and the given decay pairs indicated in subscripts, and a are specific activities of decay pairs indicated in subscripts. The r net count rates are obtained from the total and background pair events. Eqs. (1) hold for samples with atomic compositions similar to those of the calibration standards used. Eqs. (1) remain valid regardless of the state of secular equilibrium in the measured material.

In many cases, samples are close to secular equilibrium and the user may assume the following relationships

$$\begin{aligned}
 a_{Th-232} &= a_{Bi-212/Po-212} = a_{Rn-220/Po-216}, \\
 a_{U-238} &= a_{Bi-214/Po-214}, \\
 a_{U-235} &= a_{Rn-219/Po-215}, \\
 r_{\alpha} &= k_{\alpha,Th-232}a_{Th-232} + k_{\alpha,U-238}a_{U-238} \\
 &\quad + k_{\alpha,U-235}a_{U-235}, \\
 r_{\beta} &= k_{\beta,Th-232}a_{Th-232} + k_{\beta,U-238}a_{U-238} \\
 &\quad + k_{\beta,U-235}a_{U-235} + k_{\beta,K-40}a_{K-40}.
 \end{aligned} \tag{2}$$

Here r_{α} and r_{β} are the α and β net count rates. Eqs. (1) and (2) enable the calculation of the decay chain specific activities in the sample. These equations calculate the activity of pure β emitters. In (Eg. 2), it is assumed that ^{40}K is the major β contributor, which is true for most environmental samples. However, it needs to be borne in mind that in environmental samples also other β emitters can be found, e.g. natural ^{87}Rb or anthropogenic ^{137}Cs (Ochiai et al., 2018; Buesseler et al., 2015; Poręba et al., 2015; Faure and Powell, 1972; Evangeliou et al., 2014; Sanderson et al., 2016). This needs to be considered individually for each sample as it may introduce an error in the ^{40}K assessment. For example Warren (1978) gives an average ^{87}Rb at the level of 50 ppm of natural rubidium per 1% of potassium.

Eqs. (1) and (2) can be further restricted using a known $^{238}\text{U}/^{235}\text{U}$ isotopic ratio (Uvarova et al., 2014; Brennecka et al., 2010)

$$\frac{^{238}\text{U}}{^{235}\text{U}} = \frac{a_{U-238}/\lambda_{U-238}}{a_{U-235}/\lambda_{U-235}} = 137.88. \tag{3}$$

where λ is decay constant of radioisotope indicated in subscript. Eq. (3) removes one degree of freedom and allows more precise results to be obtained. In the natural environment, the ratio $^{238}\text{U}/^{235}\text{U}$ ratio can vary by up to ca. 5‰ (Uvarova et al., 2014; Brennecka et al., 2010; Placzek et al., 2016; Phan et al., 2018; Brennecka et al., 2018). This however is consistent enough to assume it is constant within measurement accuracy and precision.

2.5. System calibration

The μ Dose system needs to be calibrated with reference materials of known radioactivities, as well as a background sample. In the current work we use IAEA-RGU-1, IAEA-RGTh-1, and IAEA-RGK-1 standards from the International Atomic Energy Agency (IAEA, 1987). The IAEA-RGU-1 and IAEA-RGTh-1 are produced using uranium and thorium ores that are mixed with floated silica powder. Decay chains present in those reference materials can be considered to be in secular equilibrium with parent radioactivity. The IAEA-RGK-1 reference material is produced using high purity (99.8%) potassium sulfate. The μ Dose software contains a dedicated module that allows the user to easily obtain calibration parameters (k in Eqs. 1 and 2) by means of weighted least squares method. This is done by matching calibration measurements with known radioactivities from the built-in database.

To cite this version: Tudyka, K., Miłosz, S., Adamiec, G., Bluszcz, A., Poręba, G., Paszkowski, Ł., Kolarczyk, A. (2018) μ Dose: a compact system for environmental radioactivity and dose rate measurement. Radiation Measurements 118, 8-13 doi: doi.org/10.1016/j.radmeas.2018.07.016

Table 1: Specific radioactivity measurements using μ Dose, a HPGe and a traditional TSAC system. Given uncertainties correspond to 1σ .

	Mean ^{238}U radioactivity (Bq·kg $^{-1}$)			Mean ^{232}Th radioactivity (Bq·kg $^{-1}$)			^{40}K assessment (Bq·kg $^{-1}$)		Measurement time (hr)	
	μ Dose	TSAC	HPGe	μ Dose	TSAC	HPGe	μ Dose	HPGe	μ Dose & TSAC	HPGe
1 ^a	1620 \pm 40	2400 \pm 150	1628 \pm 32	1110 \pm 60	1300 \pm 150	1062 \pm 37	4480 \pm 160	4610 \pm 110	44	6.5
2	26.3 \pm 2.6	30.1 \pm 4.4	26.08 \pm 0.59	32 \pm 4.0	31.8 \pm 4.3	33.90 \pm 1.10	576 \pm 48	564 \pm 19	74	25
3	30.9 \pm 2.5	26.7 \pm 4.2	26.16 \pm 0.55	30.1 \pm 3.3	39.3 \pm 4.1	32.86 \pm 1.05	588 \pm 20	532 \pm 18	98	27
4	38.1 \pm 3.9	41.6 \pm 5.2	27.71 \pm 0.58	33.6 \pm 4.5	41.1 \pm 5.2	35.46 \pm 1.13	618 \pm 27	570 \pm 19	66	24
5	23.5 \pm 2.8	26.4 \pm 2.4	17.80 \pm 0.37	19.3 \pm 2.8	24.0 \pm 2.4	19.48 \pm 0.89	308 \pm 18	324 \pm 11	87	29

^a Sample created from mixing IAEA-RGU-1, IAEA-RGTh-1, and IAEA-RGK-1 in equal weight proportions. The activities calculated using reference values (IAEA, 1987) are 1673 Bq·kg $^{-1}$ of ^{238}U , 1083 Bq·kg $^{-1}$ of ^{232}Th and 4669 Bq·kg $^{-1}$ of ^{40}K .

3. Results and Discussion

3.1. Samples and sample preparation

To test the performance of μ Dose, activities of five samples were assessed using two additional systems, namely, a high-purity germanium (HPGe) γ spectrometer and a conventional TSAC system.

Sample 1 was an artificial sample composed from IAEA-RGU-1, IAEA-RGTh-1, and IAEA-RGK-1 mixed in equal weight proportions allowing the calculation of its specific activities using the IAEA reference activities. Samples 2, 3 and 4 are loess sediments. Sample 5 is a brick from archaeological excavations.

For μ Dose and TSAC, the samples were powdered using an agate mill to avoid overcounting of α particles which may arise from inhomogeneous distribution of radioactive elements in natural samples (Zöller and Pernicka, 1989; Murray, 1982; Poręba and Murray, 2006). After the milling grain size distribution was verified using a laser diffractometer Mastersizer 3000 manufactured by Malvern Instruments Ltd. For all samples the median particle size was less than 7 μm . In both μ Dose and TSAC systems, we used ground up 1 g samples and 42 mm diameter scintillators. The measurement time was the same for the μ Dose and TSAC systems. TSAC measurements were performed using an in-house built system with pulse amplitude-time analyzer Tudyka and Bluszcz (2011). The γ spectrometry measurements were performed using a low background, high resolution HPGe detector with a resolution at full width at half maximum of 1.8 keV and relative efficiency of 40% at the energy of 1332 keV manufactured by Canberra. The same standards were used as above. The average specific radioactivities were calculated using a weighted mean obtained for selected lines. The lines ^{234}Th , $^{234\text{m}}\text{Pa}$, ^{214}Pb , ^{214}Bi and ^{210}Pb were used for ^{238}U , whereas the lines of ^{228}Ac , ^{212}Pb , ^{212}Bi and ^{208}Tl were used for ^{232}Th .

3.2. Measurements

The system set-up and data were evaluated according to Aitken (1985). μ Dose specific uranium, thorium and potassium radioactivities were obtained using Eqs. (1-3).

The results and counting times are summarised in Table 1.

3.3. System performance

As seen in Table 1, there is a very good agreement between the values obtained using the μ Dose, gamma spectrometry and reference value for sample 1 (a mix of the IAEA standards - see previous subsection). In this case, the TSAC result significantly deviates from the known activities. This might be caused by a different sample reflection and a radioactivity much higher than seen in average sediment samples. For all samples, the results obtained using TSAC are characterised by larger measurement errors for the same counting times, and as mentioned earlier information on the potassium content is unavailable.

Thorium and potassium specific activities agree within 2 standard deviations between μ Dose and gamma spectrometry. Uranium specific activities for samples 4 and 5 agree within 3 standard deviations between μ Dose and gamma spectrometry. In the investigated samples, there was no indication of possible lack of secular equilibrium in the U and Th decay chains.

When the activities are used to estimate the annual dose in trapped charge dating applications it has to be borne in mind that the values and errors returned by μ Dose are correlated. This fact is taken into account during the calculation of the annual dose and leads to lower dose rate errors than in case these values were independent, as e.g. in high resolution gamma spectrometry. The calculations of annual dose will be discussed elsewhere.

4. Conclusion

The μ Dose system allows to detect α and β radiation with four different decay pairs arising in the ^{238}U decay chain ($^{214}\text{Bi}/^{214}\text{Po}$), ^{232}Th decay chain ($^{220}\text{Rn}/^{216}\text{Po}$ and $^{212}\text{Bi}/^{212}\text{Po}$) and ^{235}U decay chain ($^{219}\text{Rn}/^{215}\text{Po}$). If the sample is close enough to secular equilibrium, the obtained α and β counts and four separate decay pairs allow to obtain the ^{238}U , ^{235}U and ^{232}Th decay chains concentration in the sample. The ^{40}K activity is assessed from the excess of β counts over what is expected over what is predicted from ^{238}U , ^{235}U and ^{232}Th measurements.

μ Dose software allows for a convenient system calibration which limits routine work required from the user. The activities are calculated according to various assumptions on secular equilibrium, and measurement reports are automatically created for convenient post-processing. The μ Dose system can be equipped with various photomultipliers to assess various sample masses from 0.4–4 g. The software is build with emphasis on EPR/OSL/TL dating therefore it includes various modules for dose rate calculation.

5. Acknowledgements

The development of the pulse analyzer used in the μ Dose system was supported with the grant LIDER/001/404/L-4/2013 by the Polish National Centre for Research and Development. Currently the project is co-financed by the Polish Ministry of Science and Higher Education from "Incubator of Innovation+" programme within the framework of the Smart Growth Operational Programme, Action 4.4 Potential increase of human resources of the R&D sector.

The authors thank Ms. Agnieszka Szymak for her help in carrying out the measurements.

To cite this version: Tudyka, K., Miłosz, S., Adamiec, G., Bluszcz, A., Poręba, G., Paszkowski, Ł., Kolarczyk, A. (2018) μ Dose: a compact system for environmental radioactivity and dose rate measurement. *Radiation Measurements* 118, 8-13 doi: doi.org/10.1016/j.radmeas.2018.07.016

6. References

References

- Aitken, M., 1985. Thermoluminescence Dating. Academic Press, London.
- Bøtter-Jensen, L., Mejdahl, V., 1988. Assessment of beta dose-rate using a GM multiscaler system. *International Journal of Radiation Applications and Instrumentation. Part D. Nuclear Tracks and Radiation Measurements* 14, 187–191. URL: <https://www.sciencedirect.com/science/article/pii/1359018988900623>, doi:10.1016/1359-0189(88)90062-3.
- Brennecka, G.A., Amelin, Y., Kleine, T., 2018. Uranium isotope ratios of Muonionalusta troilite and complications for the absolute age of the IVA iron meteorite core. *Earth and Planetary Science Letters* 490, 1–10. URL: <https://www.sciencedirect.com/science/article/pii/S0012821X18301328?via%3Dihub>, doi:10.1016/J.EPSL.2018.03.010.
- Brennecka, G.A., Borg, L.E., Hutcheon, I.D., Sharp, M.A., Anbar, A.D., 2010. Natural variations in uranium isotope ratios of uranium ore concentrates: Understanding the $^{238}\text{U}/^{235}\text{U}$ fractionation mechanism. *Earth and Planetary Science Letters* 291, 228–233. URL: <http://www.sciencedirect.com/science/article/pii/S0012821X10000579?via%3Dihub#tbl1>, doi:10.1016/j.epsl.2010.01.023.
- Buesseler, K.O., German, C.R., Honda, M.C., Ohtsuka, S., Black, E.E., Kawakami, H., Manganini, S.J., Pike, S.M., 2015. Tracking the Fate of Particle Associated Fukushima Daiichi Cesium in the Ocean off Japan. *Environmental Science & Technology* 49, 9807–9816. URL: <http://pubs.acs.org/doi/10.1021/acs.est.5b02635>, doi:10.1021/acs.est.5b02635.
- Cawthra, H., Jacobs, Z., Compton, J., Fisher, E., Karkanis, P., Marean, C., 2018. Depositional and sea-level history from MIS 6 (Termination II) to MIS 3 on the southern continental shelf of South Africa. *Quaternary Science Reviews* 181, 156–172. URL: <https://www.sciencedirect.com/science/article/pii/S0277379117302081>, doi:10.1016/J.QUASCIREV.2017.12.002.
- Chen, Y., Li, S.H., Li, B., Hao, Q., Sun, J., 2015. Maximum age limitation in luminescence dating of Chinese loess using the multiple-aliquot MET-pIRIR signals from K-feldspar. *Quaternary Geochronology* 30, 207–212. URL: <https://www.sciencedirect.com/science/article/pii/S1871101415000035>, doi:10.1016/j.quageo.2015.01.002.
- Duller, G.A., Tooth, S., Barham, L., Tsukamoto, S., 2015. New investigations at Kalambo Falls, Zambia: Luminescence chronology, site formation, and archaeological significance. *Journal of Human Evolution* 85, 111–125. URL: <https://www.sciencedirect.com/science/article/pii/S0047248415001104>, doi:10.1016/J.JHEVOL.2015.05.003.
- Dunseth, Z.C., Junge, A., Lomax, J., Boaretto, E., Finkelstein, I., Fuchs, M., Shahack-Gross, R., 2017. Dating archaeological sites in an arid environment: A multi-method case study in the Negev Highlands, Israel. *Journal of Arid Environments* 144, 156–169. URL: <https://www.sciencedirect.com/science/article/pii/S014019631730109X?via%3Dihub#sec3>, doi:10.1016/J.JARIDENV.2017.05.006.
- Eitheim, E.S., May, D., Forbes, T.Z., Nelson, A.W., 2016. Disequilibrium of Naturally Occurring Radioactive Materials (NORM) in Drill Cuttings from a Horizontal Drilling Operation. *Environmental Science & Technology Letters* 3, 425–429. URL: <http://pubs.acs.org/doi/10.1021/acs.estlett.6b00439>, doi:10.1021/acs.estlett.6b00439.
- Evangelidou, N., Florou, H., Kritidis, P., 2014. A Survey of ^{137}Cs in Sediments of the Eastern Mediterranean Marine Environment from the Pre-Chernobyl Age to the Present. *Environmental Science & Technology Letters* 1, 102–107. URL: <http://pubs.acs.org/doi/10.1021/ez400078t>, doi:10.1021/ez400078t.
- Faure, G., Powell, J.L., 1972. The Geochemistry of Rubidium and Strontium, in: *Strontium Isotope Geology*. Springer Berlin Heidelberg, Berlin, Heidelberg, pp. 1–8. doi:10.1007/978-3-642-65367-4.
- Fu, X., Li, S.H., Li, B., Fu, B., 2017. A fluvial terrace record of late Quaternary folding rate of the Anjihai anticline in the northern piedmont of Tian Shan, China. *Geomorphology* 278, 91–104. URL: <https://www.sciencedirect.com/science/article/pii/S0169555X16309801>, doi:10.1016/J.GEOMORPH.2016.10.034.
- Huntley, D., 1978. The Effect of Sample Reflectance in Alpha Counting. *Ancient TL*, 2–3.
- IAEA, 1987. IAEA/RL/148. Technical Report. International Atomic Energy Agency. Vienna.
- Jacobs, Z., Jankowski, N.R., Dibble, H.L., Goldberg, P., McPherron, S.J., Sandgathe, D., Soressi, M., 2016. The age of three Middle Palaeolithic sites: Single-grain optically stimulated luminescence chronologies for Pech de l’Azé I, II and IV in France. *Journal of Human Evolution* 95, 80–103. URL: <http://linkinghub.elsevier.com/retrieve/pii/S0047248416300021>, doi:10.1016/j.jhevol.2016.03.010.

To cite this version: Tudyka, K., Miłosz, S., Adamiec, G., Bluszcz, A., Poręba, G., Paszkowski, L., Kolarczyk, A. (2018) μ Dose: a compact system for environmental radioactivity and dose rate measurement. *Radiation Measurements* 118, 8-13 doi: doi.org/10.1016/j.radmeas.2018.07.016

- Jankowski, N.R., Gully, G.A., Jacobs, Z., Roberts, R.G., Prideaux, G.J., 2016. A late Quaternary vertebrate deposit in Kudjal Yolgah Cave, south-western Australia: refining regional late Pleistocene extinctions. *Journal of Quaternary Science* 31, 538–550. URL: <https://onlinelibrary.wiley.com/doi/abs/10.1002/jqs.2877><http://doi.wiley.com/10.1002/jqs.2877>, doi:10.1002/jqs.2877.
- Junge, A., Lomax, J., Shahack-Gross, R., Dunseth, Z.C., Finkelstein, I., Fuchs, M., 2016. OSL Age Determination of Archaeological Stone Structures Using Trapped Aeolian Sediments: A Case Study from the Negev Highlands, Israel. *Geoarchaeology* 31, 550–563. URL: <https://onlinelibrary.wiley.com/doi/abs/10.1002/gea.21578><http://doi.wiley.com/10.1002/gea.21578>, doi:10.1002/gea.21578.
- Krbetschek, M., Rieser, U., Zöller, L., Heinicke, J., 1994. Radioactive disequilibria in palaeodosimetric dating of sediments. *Radiation Measurements* 23, 485–489. URL: <https://www.sciencedirect.com/science/article/pii/1350448794900833>, doi:10.1016/1350-4487(94)90083-3.
- Kühn, P., Lehnendorff, E., Fuchs, M., 2017. Lateglacial to Holocene pedogenesis and formation of colluvial deposits in a loess landscape of Central Europe (Wetterau, Germany). *CATENA* 154, 118–135. URL: <https://www.sciencedirect.com/science/article/pii/S0341816217300668?via%3Dihub>, doi:10.1016/J.CATENA.2017.02.015.
- Miłosz, S., Tudyka, K., Walencik-Łata, A., Barwinek, S., Bluszcz, A., Adamiec, G., 2017. Pulse Height, Pulse Shape, and Time Interval Analyzer for Delayed α/β Coincidence Counting. *IEEE Transactions on Nuclear Science* 64, 2536–2542. URL: <http://ieeexplore.ieee.org/document/7990600/>, doi:10.1109/TNS.2017.2731852.
- Murray, A.S., 1982. Studies of the stability of radioisotope concentrations and their dependence on grain size. *PACT* 6, 216–223.
- Ochiai, A., Imoto, J., Suetake, M., Komiya, T., Furuki, G., Ikehara, R., Yamasaki, S., Law, G.T.W., Ohnuki, T., Grambow, B., Ewing, R.C., Utsunomiya, S., 2018. Uranium Dioxides and Debris Fragments Released to the Environment with Cesium-Rich Microparticles from the Fukushima Daiichi Nuclear Power Plant. *Environmental Science & Technology* 52, 2586–2594. URL: <http://pubs.acs.org/doi/10.1021/acs.est.7b06309>, doi:10.1021/acs.est.7b06309.
- Phan, T.T., Gardiner, J.B., Capo, R.C., Stewart, B.W., 2018. Geochemical and multi-isotopic ($^{87}\text{Sr}/^{86}\text{Sr}$, $^{143}\text{Nd}/^{144}\text{Nd}$, $^{238}\text{U}/^{235}\text{U}$) perspectives of sediment sources, depositional conditions, and diagenesis of the Marcellus Shale, Appalachian Basin, USA. *Geochimica et Cosmochimica Acta* 222, 187–211. URL: <https://www.sciencedirect.com/science/article/pii/S0016703717306841?via%3Dihub>, doi:10.1016/J.GCA.2017.10.021.
- Placzek, C.J., Heikoop, J.M., House, B., Linhoff, B.S., Pelizza, M., 2016. Uranium isotope composition of waters from South Texas uranium ore deposits. *Chemical Geology* 437, 44–55. URL: <https://www.sciencedirect.com/science/article/pii/S0009254116302376#bbb0035>, doi:10.1016/J.CHEMGEO.2016.05.008.
- Poręba, G.J., Murray, A., 2006. Sediment tracing using environmental radionuclides; the distribution and behaviour of ^{137}Cs and natural radioisotopes in a small loess agricultural watershed. *Ecohydrology & Hydrobiology* 6, 153–161. URL: <http://linkinghub.elsevier.com/retrieve/pii/S1642359306701379>, doi:10.1016/S1642-3593(06)70137-9.
- Poręba, G.J., Śnieszko, Z., Moska, P., 2015. Application of OSL dating and ^{137}Cs measurements to reconstruct the history of water erosion: A case study of a Holocene colluvium in Świerklany, south Poland. *Quaternary International* 374, 189–197. URL: <https://www.sciencedirect.com/science/article/pii/S1040618215002578>, doi:10.1016/j.quaint.2015.04.004.
- Prescott, J., Hutton, J., 1995. Environmental dose rates and radioactive disequilibrium from some Australian luminescence dating sites. *Quaternary Science Reviews* 14, 439–448. URL: <https://www.sciencedirect.com/science/article/pii/0277379195000372>, doi:10.1016/0277-3791(95)00037-2.
- Roettig, C.B., Kolb, T., Wolf, D., Baumgart, P., Richter, C., Schleicher, A., Zöller, L., Faust, D., 2017. Complexity of Quaternary aeolian dynamics (Canary Islands). *Palaeogeography, Palaeoclimatology, Palaeoecology* 472, 146–162. URL: <https://www.sciencedirect.com/science/article/pii/S0031018216304151?via%3Dihub>, doi:10.1016/J.PALAEO.2017.01.039.
- Sabtu, S.N., Mahat, R.H., Amin, Y.M., Price, D.M., Bradley, D., Maah, M.J., 2015. Thermoluminescence dating analysis at the site of an ancient brick structure at Pengkalan Bujang, Malaysia. *Applied Radiation and Isotopes* 105, 182–187. URL: <https://www.sciencedirect.com/science/article/pii/S0969804315301640><http://linkinghub.elsevier.com/retrieve/pii/S0969804315301640>, doi:10.1016/j.apradiso.2015.08.024.
- Sanderson, D., 1988. Thick source beta counting (TSBC): A rapid method for measuring beta dose-rates. *International Journal of Radiation Applications and Instrumentation. Part D. Nuclear Tracks and Radiation Measurements* 14, 203–207. URL: <http://linkinghub.elsevier.com/retrieve/pii/1359018988900659>, doi:10.1016/1359-0189(88)90065-9.

To cite this version: Tudyka, K., Miłosz, S., Adamiec, G., Bluszcz, A., Poręba, G., Paszkowski, Ł., Kolarczyk, A. (2018) μ Dose: a compact system for environmental radioactivity and dose rate measurement. *Radiation Measurements* 118, 8-13 doi: doi.org/10.1016/j.radmeas.2018.07.016

- Sanderson, D., Cresswell, A., Tamura, K., Iwasaka, T., Matsuzaki, K., 2016. Evaluating remediation of radionuclide contaminated forest near Iwaki, Japan, using radiometric methods. *Journal of Environmental Radioactivity* 162-163, 118–128. URL: <https://www.sciencedirect.com/science/article/pii/S0265931X16301631?via%3DiHub>, doi:10.1016/J.JENVRAD.2016.05.019.
- Schmidt, C., Schaarschmidt, M., Kolb, T., Büchel, G., Richter, D., Zöller, L., 2017. Luminescence dating of Late Pleistocene eruptions in the Eifel Volcanic Field, Germany. *Journal of Quaternary Science* 32, 628–638. URL: <http://doi.wiley.com/10.1002/jqs.2961>, doi:10.1002/jqs.2961.
- Tudyka, K., Bluszcz, A., 2011. Very low cost multichannel analyzer with some additional features. *Nuclear Instruments and Methods in Physics Research, Section A: Accelerators, Spectrometers, Detectors and Associated Equipment* 659, 419–421. doi:10.1016/j.nima.2011.09.015.
- Tudyka, K., Miłosz, S., Ustrzycka, A., Barwinek, S., Barwinek, W., Walencik-Lata, A., Adamiec, G., Bluszcz, A., 2017. A low level liquid scintillation spectrometer with five counting modules for ^{14}C , ^{222}Rn and delayed coincidence measurements. *Radiation Measurements* 105, 1–6. URL: <http://linkinghub.elsevier.com/retrieve/pii/S1350448716304139>, doi:10.1016/j.radmeas.2017.06.003.
- Turner, R., Radley, J., Mayneord, W., 1958. The alpha-ray activity of human tissues. *British Journal of Radiology* 31, 397–402.
- Uvarova, Y.A., Kyser, T.K., Geagea, M.L., Chipley, D., 2014. Variations in the uranium isotopic compositions of uranium ores from different types of uranium deposits. *Geochimica et Cosmochimica Acta* 146, 1–17. URL: <https://www.sciencedirect.com/science/article/pii/S0016703714005924#t0010>, doi:10.1016/j.gca.2014.09.034.
- Warren, S.E., 1978. THERMOLUMINESCENCE DATING OF POTTERY: AN ASSESSMENT OF THE DOSE-RATE FROM RUBIDIUM. *Archaeometry* 20, 71–72. URL: <http://doi.wiley.com/10.1111/j.1475-4754.1978.tb00215.x>, doi:10.1111/j.1475-4754.1978.tb00215.x.
- Zöller, L., Pernicka, E., 1989. A note on overcounting in alpha-counters and its elimination. *Ancient TL*, 11–14.